

# Faster Minimization of Linear Wirelength for Global Placement

Charles J. Alpert, *Member, IEEE*, Tony F. Chan, Andrew B. Kahng, *Associate Member, IEEE*,  
Igor L. Markov, *Student Member, IEEE*, and Pep Mulet, *Member, IEEE*

**Abstract**—A linear wirelength objective more effectively captures timing, congestion, and other global placement considerations than a squared wirelength objective. The GORDIAN-L cell placement tool [19] minimizes linear wirelength by first approximating the linear wirelength objective by a modified squared wirelength objective, then executing the following loop—1) minimize the current objective to yield some approximate solution and 2) use the resulting solution to construct a more accurate objective—until the solution converges. This paper shows how to apply a generalization [5], [6] of a 1937 algorithm due to Weiszfeld [22] to placement with a linear wirelength objective and that the main GORDIAN-L loop is actually a special case of this algorithm. We then propose applying a regularization parameter to the generalized Weiszfeld algorithm to control the tradeoff between convergence and solution accuracy; the GORDIAN-L iteration is equivalent to setting this regularization parameter to zero. We also apply novel numerical methods, such as the primal-Newton and primal-dual Newton iterations, to optimize the linear wirelength objective. Finally, we show both theoretically and empirically that the primal-dual Newton iteration stably attains quadratic convergence, while the generalized Weiszfeld iteration is linear convergent. Hence, primal-dual Newton is a superior choice for implementing a placer such as GORDIAN-L, or for any linear wirelength optimization.

**Index Terms**—Analytic placement, GORDIAN-L, interconnect delay, linear placement, linear wirelength, Newton, primal dual, quadratic placement, Weiszfeld.

## I. INTRODUCTION

THE placement phase of layout has a significant impact on routability and performance of a given IC design. Quadratic placement techniques have received wide attention over the past decade, since they are efficient enough to handle large designs while retaining good solution quality. The quadratic placement approach can be traced back to [3], [8], [21], [23], and other early works. The basic idea is to solve recursively generated sparse systems of linear equations, where each system captures a one-dimensional (1-D) placement problem with minimum squared wirelength objective. The solution to any given 1-D placement can be refined in

various ways, e.g., the PROUD algorithm of [21] applies min-cut partitioning to induce hierarchical subproblems, and the GORDIAN algorithm of [13] applies min-cut partitioning as well as center-of-gravity constraints that define a more constrained version of the original problem.

The heart of the quadratic placement technique lies in solving for the 1-D placements. Two such placements in the  $x$ - and  $y$ -directions will induce a two-dimensional (2-D) “global placement,” which due to the objective function and continuous formulation will have most cells clumped in the center of the layout region. Quadratic placers vary mostly in how they map a global placement to a feasible cell placement (i.e., with nonoverlapped cells in legal locations). Min-cut partitioning and center-of-gravity constraints are simply a means of gradually “spreading out” the global placement during the course of this mapping. The well-known example of GORDIAN [13] uses a conjugate-gradient iteration to solve for optimal cell locations under the squared wirelength objective then partitions the cells by assigning each cell to one of four centers of gravity that correspond to the four quadrants of the layout. Constraints are defined such that all cells assigned to a given center of gravity must have average  $x$ - and  $y$ -coordinates at that location. The numerical optimization is performed again with the added constraints and each quadrant is subdivided into four subquadrants. GORDIAN terminates when each cell has been assigned to a unique center of gravity.

Observe that the squared wirelength objective is applied only because it allows the 1-D placement problem to be reduced to the solution of a system of linear equations. The main difficulty with the squared wirelength objective is that it overpenalizes long wires and underpenalizes short wires. Thus, a strongly connected cluster may be spread out over the placement, which increases wiring congestion for the router. The extra wiring caused by the spread of highly connected components can also reduce the routing resource flexibility needed to satisfy timing and signal integrity constraints.

Mahmoud *et al.* [16] have compared the linear and squared wirelength objectives for analog placement and concluded that the linear wirelength objective is superior. Indeed, whenever a more “detailed” placement objective is feasible, as with simulated annealing approaches [20], the preferred objective has always been based on minimum spanning tree, single-trunk Steiner tree, or bounding-box perimeter routing estimates. Such routing estimates reflect linear wirelength and more accurately capture congestion (routing resource utilization) and

Manuscript received June 20, 1997. An earlier version of this paper was presented at ISPD-97. This work was supported by a grant from Cadence Design Systems, San Jose, CA 95134 USA. This paper was recommended by Associate Editor M. Sarrafzadeh.

C. J. Alpert is with the IBM Austin Research Laboratory, Austin, TX 78758 USA (e-mail: alpert@austin.ibm.com).

T. F. Chan, I. L. Markov, and P. Mulet are with the Mathematics Department, University of California, Los Angeles 90095 USA.

A. B. Kahng is with the Computer Science Department, University of California, Los Angeles 90095 USA.

Publisher Item Identifier S 0278-0070(98)02052-1.

interconnect-related signal delay.<sup>1</sup> Works such as [18] have further shown that a linear wirelength objective can be used to form 1-D placements that directly yield effective bipartitioning solutions.

The 1991 work of Sigl *et al.* [19] proposed an important modification of GORDIAN, called GORDIAN-L, which optimizes the linear wirelength objective.<sup>2</sup> Since the linear wirelength objective cannot be addressed directly by numerical methods, GORDIAN-L approximates the linear objective by a quadratic objective, then executes the following loop: 1) minimize the current quadratic objective to yield some approximate solution and 2) use this solution to find a better quadratic objective until the solution converges. GORDIAN-L achieves solutions with up to 20% less area than GORDIAN while significantly reducing routing density and total minimum spanning tree cost [19]; it has been used widely in industry for both ASIC and structured-custom design (e.g., Motorola PrediX floorplanner, Siemens LINPLACE placer, etc.). However, the GORDIAN-L improvement comes at the price of significantly increased central processing unit (CPU) cost ([19] reports a factor of five increase over GORDIAN). To achieve reduced CPU cost, or substantially improved solution accuracy within given CPU cost bounds, our work has developed alternative numerical methods for linear wirelength minimization.

The purpose of our paper is to apply new numerical methods to the problem of analytic very large scale integration (VLSI) placement with a linear wirelength objective. Our contributions are as follows.

- We show that the main GORDIAN-L loop can be viewed as a special case of a generalized version [5], [6] of a 1937 algorithm due to Weiszfeld [24]. This relationship allows us to extend the technique to other objectives.
- The GORDIAN-L solver uses a technique called *minimal gate width* (cf., p. 429 of the original GORDIAN-L paper [19]) to avoid numerical errors when the distance between two placed objects is close to zero. While we can use the minimal gate width with generalized Weiszfeld, we instead propose using a  $\beta$ -regularization parameter to control the tradeoff between convergence and solution accuracy. We show that the original GORDIAN-L iteration with zero minimal gate width is equivalent to setting  $\beta$  equal to zero.

<sup>1</sup>Recent literature has noted that a first-moment  $RC$  delay estimate such as Elmore delay [7] has a term that is quadratic in the length of a source-sink routing path. In performance-driven deep-submicron design, this fact needs to be taken into some perspective. We observe that a local net [say,  $O(100)$   $\mu\text{m}$  in length] will typically be driven by a small device and routed on high-impedance lower routing layers: when the driver resistance is high, the dominant portion of interconnect-related delay is from capacitive loading, i.e., it is linearly dependent on total wirelength. On the other hand, a (timing-critical) global net [say,  $O(1000)$   $\mu\text{m}$  in length] will be driven by a larger device and routed (with appropriate spacing and topology) on wider, lower-impedance upper layers. Even if the ratio of driver/wire resistances is low enough for wire resistance effects to become significant, design methodology such as repeater insertion (needed to reduce gate load delay and improve noise immunity, as well as reduce interconnect delay) and wire width sizing will yield interconnect-related delay that is more “linear” than “quadratic.”

<sup>2</sup>More recent works also discuss the linear wirelength objective. Notably, Li *et al.* [14] use spectral techniques and clustering to address a combination of the linear and squared wirelength objectives; see also [10].

- We note that our generalization of GORDIAN-L can handle not only linear wirelength, but also wirelength of an arbitrary real exponent  $p \geq 1$ .
- Next, we apply modern numerical methods such as primal Newton and primal-dual Newton to placement with a linear wirelength objective. While such methods have been previously used in fields such as image processing, our work is the first to mathematically derive how such methods can be applied to the linear wirelength placement objective. We further show that primal-dual Newton stably attains quadratic convergence, thus improving substantially over the linearly convergent Weiszfeld iteration. Primal-dual Newton solves the same problem that the GORDIAN-L engine solves, except that it is more general (thus enabling other placement formulations).
- Extensive experiments show that primal-dual Newton converges significantly faster than the Weiszfeld (GORDIAN-L) solver over a range of instance complexities and  $\beta$ -regularization regimes. It is straightforward to integrate the primal-dual Newton iteration into existing numerical placement engines.

## II. PRELIMINARIES

A quadratic placer takes a netlist hypergraph as input and produces a placement of the cells. To apply existing numerical optimizations, the netlist must first be transformed into a graph.

*Definition:* An *undirected weighted graph*  $G(V, E)$  consists of a set of vertices  $V = \{v_1, v_2, \dots, v_n\}$  and a set of edges  $E = \{e_1, e_2, \dots, e_m\}$  where each edge is an unordered pair of vertices. A weight function  $w: E \rightarrow \mathbb{R}^+$  assigns a nonnegative weight  $w(e)$  to each edge  $e$ .

To convert the netlist into a graph, the authors of [13] use a *star model* wherein a new “net node” is created for each net in the netlist, and an edge is added between the net node and each cell connected to the net. Placing the net node at the center of its incident cells (as GORDIAN assumes) makes the star model equivalent to a *clique model* which introduces an edge of weight  $2/p$  between every pair of cells incident to a given  $p$ -pin net. The total squared wirelength will be the same for any placement under either the star or clique models.

*Definition:* The  $n \times n$  *adjacency matrix*  $\mathbf{A} = (a_{ij})$  for the graph  $G$  has entry  $a_{ij} = w(v_i, v_j)$  if  $(v_i, v_j) \in E$  and  $a_{ij} = 0$  otherwise.

*Definition:* The  $n \times n$  *Laplacian matrix*  $\mathbf{Q} = (q_{ij})$  of  $\mathbf{A}$  has entry  $q_{ij}$  equal to  $-a_{ij}$  if  $i \neq j$  and entry  $q_{ii}$  equal to  $\sum_{j=1}^n a_{ij}$ , i.e.,  $q_{ii}$  is the *degree* of vertex  $v_i$ .

*Definition:* The  $n$ -dimensional *placement vector*  $\mathbf{x} = (x_i)$  corresponds to the physical locations of cells  $v_1, \dots, v_n$  on the real line, i.e.,  $x_i$  is the coordinate of vertex  $v_i$ .

GORDIAN [13] uses a squared wirelength objective.

**Squared Wirelength Formulation:** Minimize

$$\Phi_Q(\mathbf{x}) = \frac{1}{2} \mathbf{x}^T \mathbf{Q} \mathbf{x} + \mathbf{d}^T \mathbf{x} = \sum_{i>j}^n a_{ij} (x_i - x_j)^2 + \mathbf{d}^T \mathbf{x}$$

s.t.  $\mathbf{H} \mathbf{x} = \mathbf{b}$ . (1)

Here,  $\mathbf{H}$  is a  $q \times n$  *constraint matrix* that represents  $q$  center of gravity constraints [a special case is that of fixed (pad)

locations]. Vector  $\mathbf{b}$  gives the coordinates of the  $q$  centers of gravity. For  $v_j$  belonging to the  $i$ th group of vertices, the  $(i, j)$  entry of  $\mathbf{H}_x$  is set to be  $1/n_i$ , where  $n_i$  is the total number of vertices in the group. The optional linear term  $\mathbf{d}^T \mathbf{x}$  represents connections of cells to fixed I/O pads. The vector  $\mathbf{d}$  can also capture pin offsets [19].

*Definition:* The  $m \times n$  incidence matrix  $\mathbf{C} = (c_{ki})$  for  $G$  represents the relationship between edges and vertices of  $G$ . For each edge  $e_k = (v_i, v_j) \in E$ ,  $c_{ki} = w(e_k)$  and  $c_{kj} = -w(e_k)$ ; the orientation of edges (signs of  $c_{ki}$  and  $c_{kj}$ ) can be arbitrary. All other entries of  $\mathbf{C}$  are zero.

Note that there are  $2m$  nonzero entries in  $\mathbf{C}$  and that each row sum is zero. The GORDIAN-L linear wirelength objective is as follows.

**Linear Wirelength Formulation:** Minimize

$$\Phi_L(\mathbf{x}) = \|\mathbf{C}\mathbf{x}\|_1 = \sum_{i>j}^n a_{ij} |x_i - x_j| \quad \text{s.t. } \mathbf{H}\mathbf{x} = \mathbf{b}. \quad (2)$$

A term  $\mathbf{d}^T \mathbf{x}$  can again be added to incorporate pin offsets and connections to pads.

### III. GORDIAN AND GORDIAN-L

GORDIAN [13] obtains a placement by repeatedly optimizing  $\Phi_Q$ , alternating between the horizontal and vertical directions. Constraints for the optimizations are respectively given by  $\mathbf{H}_x \mathbf{x} = \mathbf{b}_x$  and  $\mathbf{H}_y \mathbf{y} = \mathbf{b}_y$ , corresponding to the  $x$  and  $y$  directions as explained above. To handle nonunit areas  $a(v_i)$  for each vertex  $v_i$ , entry  $ij$  can be changed to  $a(v_i)/A_j$  where  $A_j$  is the sum of the areas of all vertices with center of gravity  $b_j$ .

The algorithm must ensure that at each iteration  $\mathbf{H}_x$  and  $\mathbf{H}_y$  have maximal rank and constrain each cell by exactly one center of gravity. This implies that there is exactly one nonzero element in each column of  $\mathbf{H}_x$  and  $\mathbf{H}_y$ .

GORDIAN begins with each cell attracted to the same center of gravity located in the center of the layout. During an iteration, for each center of gravity we consider the group of cells (if of size  $\geq 2$ , i.e., if the constraint is nontrivial) attracted to it. The corresponding region is cut in two by a vertical or horizontal line passing through the center of gravity, and two new groups of cells with respective new centers of gravity replace the old group. This leads to a final solution where cells do not overlap.

Fig. 1 summarizes the flow of the GORDIAN algorithm. The algorithm takes as input a graph  $G$  obtained by applying the  $2/p$ -clique model to a circuit netlist; it outputs the coordinates of the placed cells. The **repeat** loop in Steps 2–8 continues as long as the number of cells is larger than the number of center of gravity constraints. At each iteration, Step 3 minimizes a quadratic objective function which is derived below. The resulting placement is used to refine the center of gravity constraints, yielding left and right constraints and larger linear systems (Steps 5 and 6). This process is then repeated in the  $y$  direction (Step 7), with each nontrivial constraint refined into top and bottom constraints. In each iteration, the number of subregions can quadruple, so the

---

#### GORDIAN Placement Algorithm

---

**Input:** Graph  $G(V, E)$  representing a circuit netlist, and its Laplacian  $\mathbf{Q}$ ; Offset vectors  $\mathbf{d}_x, \mathbf{d}_y$

**Output:** Vectors  $\mathbf{x}, \mathbf{y}$  denoting the vertex coordinates

**Variables:** Constraint systems  $\mathbf{H}_x \mathbf{x} = \mathbf{b}_x, \mathbf{H}_y \mathbf{y} = \mathbf{b}_y$  of increasing size representing current set of center of gravity constraints

---

1. Set  $\mathbf{b}_x$  and  $\mathbf{b}_y$  to 1-dim vectors  $c_x$  and  $c_y$  where  $(c_x, c_y)$  is the center of the layout  
Set up the objectives  
 $\Phi_Q(\mathbf{x}) = \mathbf{x}^T \mathbf{Q} \mathbf{x} + \mathbf{d}_x^T \mathbf{x}$  and  $\Phi_Q(\mathbf{y}) = \mathbf{y}^T \mathbf{Q} \mathbf{y} + \mathbf{d}_y^T \mathbf{y}$
  2. **repeat** (Steps 3-7)
  3. Minimize  $\Phi_Q(\mathbf{x})$  s.t.  $\mathbf{H}_x \mathbf{x} = \mathbf{b}_x$
  4. **for each non-trivial constraint do** (Steps 5-6)
  5. Replace with two new constraints:  
the cells to the left from the center are attracted to the center of the left half of the region. Similarly, for those cells to the right from the center. Update  $\mathbf{H}_x, \mathbf{H}_y$
  6. Replace the center of gravity  $b_i$  with centers of gravity of two new groups (update  $\mathbf{b}_x$  and  $\mathbf{b}_y$ )
  7. Repeat Steps 3-6 for  $y$  instead of  $x$  (in Step 5 use *top/bottom* instead of *left/right*)
  8. **until** no two cells share the same center of gravity
  9. **return**  $\mathbf{x}, \mathbf{y}$
- 

Fig. 1. The GORDIAN solver.

number of iterations through the **repeat** loop in Step 2 is  $O(\log n)$ .

We find the unique minimizer  $\mathbf{x}$  for  $\Phi_Q(\mathbf{x})$  defined in (1) by solving the possibly undetermined constraint system  $\mathbf{H}\mathbf{x} = \mathbf{b}$  passing to an unconstrained formulation and finally solving a quadratic programming problem as follows. Matrix  $\mathbf{H}$  is diagonalized by a permutation of columns into  $[\mathbf{H}_d | \mathbf{H}_i]$  [ $\mathbf{H}_d$  is  $q \times q$ -diagonal;  $\mathbf{H}_i$  has size  $q \times (n - q)$ ]. This diagonalization is possible since every column has exactly one nonzero element and the constraints are nondegenerate. Correspondingly, the placement vector  $\mathbf{x}$  splits into  $n - q$  independent variables  $\mathbf{x}_i$  and  $q$  dependent variables  $\mathbf{x}_d$ , so that we can rewrite  $\mathbf{H}\mathbf{x} = \mathbf{b}$  as  $[\mathbf{H}_d | \mathbf{H}_i] \begin{bmatrix} \mathbf{x}_d \\ \mathbf{x}_i \end{bmatrix} = \mathbf{b}$  or  $\mathbf{H}_d \mathbf{x}_d + \mathbf{H}_i \mathbf{x}_i = \mathbf{b}$ .

Inverting the diagonal matrix, we get

$$\mathbf{x}_d = -\mathbf{H}_d^{-1} \mathbf{H}_i \mathbf{x}_i + \mathbf{H}_d^{-1} \mathbf{b}.$$

This allows us to express  $\mathbf{x}$  as

$$\mathbf{x} = \begin{bmatrix} \mathbf{x}_d \\ \mathbf{x}_i \end{bmatrix} = \begin{bmatrix} -\mathbf{H}_d^{-1} \mathbf{H}_i \\ \mathbf{I} \end{bmatrix} \mathbf{x}_i + \begin{bmatrix} \mathbf{H}_d^{-1} \mathbf{b} \\ \mathbf{0} \end{bmatrix}$$

or as  $\mathbf{x} = \mathbf{Z}\mathbf{x}_i + \zeta$  with obvious notation for  $\mathbf{Z}$  and  $\zeta$ . We combine this formula with (1) to reduce the dimension of the unknown minimizer and obtain an unconstrained formulation

$$\Phi_Q(\mathbf{x}) = \frac{1}{2} \mathbf{x}_i^T \mathbf{Z}^T \mathbf{Q} \mathbf{Z} \mathbf{x}_i + (\mathbf{Q}\zeta + \mathbf{d})^T \mathbf{Z}^T \mathbf{x}_i + C$$

where  $C$  represents all constant terms. As  $\Phi_Q(\mathbf{x})$  depends on  $\mathbf{x}_i$  only, we introduce  $\Psi_Q(\mathbf{x}_i) = \Phi_Q(\mathbf{x})$ , so that

$$\Psi_Q(\mathbf{x}_i) = \frac{1}{2} \mathbf{x}_i^T \mathbf{Z}^T \mathbf{Q} \mathbf{Z} \mathbf{x}_i + \mathbf{c}_0^T \mathbf{Z}^T \mathbf{x}_i + C$$

where  $\mathbf{c}_0 = \mathbf{Q}\zeta + \mathbf{d}$ . We see now that  $\Psi(\mathbf{x}_i)$  gives an  $(n - q)$ -dimensional unconstrained quadratic programming problem.

To determine its optimal solution, the gradient  $\nabla\Psi(\mathbf{x}_i)$  is set to zero, yielding the  $(n - q) \times (n - q)$  linear system

$$\mathbf{Z}^T \mathbf{Q} \mathbf{Z} \mathbf{x}_i = -\mathbf{c}$$

which can be efficiently solved with, e.g., conjugate gradient or another Krylov subspace solver [9]. Once the optimal value  $\mathbf{x}_i$  is obtained, the optimal solution for  $\mathbf{x}$  is given by  $\mathbf{x} = \mathbf{Z} \mathbf{x}_i + \zeta$ .

**GORDIAN-L:** Placement with minimum squared wire-length objective has a unique solution that can be found by solving the corresponding linear system. In contrast, placement with a minimum linear wirelength objective can have multiple optimal solutions. For example, a single movable cell connected to two fixed pads by edges of equal weight can be optimally placed anywhere between the two pads. In general, the set of optimal placements is closed and lies within the convex hull of fixed pads (see [21]). Direct minimization of a linear objective function can be achieved by linear programming, but this is usually computationally expensive.

Sigl *et al.* [19] minimize the linear wirelength objective  $\Phi_L(\mathbf{x})$  by repeatedly applying the GORDIAN quadratic solver. They observe that the linear objective can be rewritten as

$$\Phi_L(\mathbf{x}) = \sum_{(i,j) \in E} a_{ij} |x_i - x_j| = \sum_{(i,j) \in E} \frac{a_{ij} (x_i - x_j)^2}{|x_i - x_j|}.$$

If  $|x_i - x_j|$  were constant in the denominator of the last term, then a quadratic objective would be obtained and could be handled easily. The GORDIAN-L solver first solves the system  $\Phi_Q(\mathbf{x})$  to obtain a reasonable approximation for each  $|x_i - x_j|$  term. Call this solution  $\mathbf{x}^0$ . GORDIAN-L then derives successively improved solutions  $\mathbf{x}^1, \mathbf{x}^2, \dots$  until there is no significant difference between  $\mathbf{x}^k$  and  $\mathbf{x}^{k-1}$ . From a given solution  $\mathbf{x}^{k-1}$ , the next solution  $\mathbf{x}^k$  is obtained by minimizing

$$\begin{aligned} \Phi_L^k(\mathbf{x}^k) &= \sum_{(i,j) \in E} \frac{a_{ij} (x_i^k - x_j^k)^2}{|x_i^{k-1} - x_j^{k-1}|} \\ &= \sum_{(i,j) \in E} g_{ij}^k \cdot (x_i^k - x_j^k)^2 \end{aligned} \quad (3)$$

where  $g_{ij}^k = a_{ij} / (|x_i^{k-1} - x_j^{k-1}|)$ . Note that the coefficients  $g_{ij}^k$  are adjusted between iterations. The iterations terminate when the factors  $(x_i^k - x_j^k)$  no longer change significantly.<sup>3</sup> Just as with  $\Phi_Q(\mathbf{x})$ , we can minimize  $\Phi_L^k(\mathbf{x})$  in (3) by applying a Krylov subspace solver.

The GORDIAN algorithm can be transformed into GORDIAN-L by replacing Step 3 of Fig. 1 with the solver shown in Fig. 2. Note that GORDIAN-L [19] also includes an additional modification. Rather than subdivide each region into two subregions, GORDIAN-L subdivides each region into *three* subregions and then minimizes the objective  $\Phi_L$ ; the result is then used to subdivide the region into *five* subregions and the minimization is performed again. The resulting solution is used as the output for Step 3 in Fig. 1 and centers of gravity are assigned as before. This modification

<sup>3</sup>Some convergence criterion must be specified in any implementation. We do not know the convergence criterion used in GORDIAN-L, which makes CPU time comparisons impossible.

### GORDIAN-L Solver (new Step 3 for Figure 1)

**Input:** Adjacency matrix  $\mathbf{A}$ , constraint matrix  $\mathbf{H}_\mathbf{x}$  and vector  $\mathbf{b}_\mathbf{x}$ .

**Output:** Solution  $\mathbf{x}$  that optimizes  $\Phi_L(\mathbf{x})$  such that  $\mathbf{H}_\mathbf{x} = \mathbf{b}_\mathbf{x}$ .

**Variables:** Intermediate solutions  $\mathbf{x}^k$

1. Solve  $\Phi(\mathbf{x}^{(0)})$  as in Step 3 of Figure 1. Set  $k = 1$ .
2. **do** (Steps 3-7)
3. Update each edge weight  $g_{ij}^k$  to  $\frac{a_{ij}}{|x_i^{k-1} - x_j^{k-1}|}$ .
4. Construct  $\Phi_L^k(\mathbf{x}^k)$  from Equation (3).
5. Minimize  $\Phi_L^k(\mathbf{x}^k)$  s.t.  $\mathbf{H}_\mathbf{x} \mathbf{x}^k = \mathbf{b}_\mathbf{x}$ .
6.  $k = k + 1$ .
7. **while**  $\sum_{1 \leq i < j \leq n} |x_i^k - x_j^{k-1}| > \epsilon$
8. **return**  $\mathbf{x}^k$ .

Fig. 2. The GORDIAN-L solver.

improves performance but also increases the number of calls to the numerical solver.

## IV. APPLYING THE WEISZFELD ALGORITHM TO PLACEMENT

In 1937, Weiszfeld [22] proposed a technique to optimize the placement of nodes in which the instance is a complete unweighted graph. In other words, the objective function is to minimize the total sum of distances between all placed objects. Later Eckhardt [5], [6] generalized this technique for arbitrary connectivity matrices. Eckhardt proves the global *linear*<sup>4</sup> convergence of this technique (see also [15]).

We show that by choosing the appropriate matrix, Eckhardt's extension of the Weiszfeld algorithm is actually equivalent to GORDIAN-L (with an initial assumption of zero minimal gate width, as opposed to a small fixed minimal gate width). This enables us to apply Eckhardt's linear convergence proof to GORDIAN-L. To guarantee numerical stability, a technique called  $\beta$ -regularization is used in the Weiszfeld algorithm.

### A. Generalized Weiszfeld Algorithm in the Context of GORDIAN-L

We now explain the generalized Weiszfeld algorithm in the context of the GORDIAN-L numerical solver. The objective is to minimize  $f(\mathbf{x}) = \|\mathbf{C}\mathbf{x}\|_1$  subject to  $\mathbf{H}\mathbf{x} = \mathbf{b}$  with the  $q \times n$ -matrix  $\mathbf{H}$  imposing  $q$  constraints on  $n$  cell locations. Observe that

$$f(\mathbf{x}) = \|\mathbf{C}\mathbf{x}\|_1 = \sum_{j=1}^m |\mathbf{C}_j \mathbf{x}| \approx \sum_{j=1}^m \sqrt{(\mathbf{C}_j \mathbf{x})^2 + \beta}$$

where  $\beta > 0$  is a small constant. The purpose of  $\beta$  is to approximate the nondifferentiable objective function by a smooth function. In order to write the derivative of  $f(\mathbf{x})$  compactly, notice that<sup>5</sup>

$$\frac{d(|\mathbf{C}_j \mathbf{x}|^2)}{d\mathbf{x}} = 2\mathbf{C}_j^T \mathbf{C}_j \mathbf{x}. \quad (4)$$

<sup>4</sup>Choose a norm and let  $\epsilon(k)$  denote the norm of the residual vector at the  $k$ th iteration. Assume that  $\log[\epsilon(0)/\epsilon(k)] \approx Bk^s$  for some constant  $B$  and  $s \in \{1, 2\}$ . We say that the convergence is *linear* when  $s = 1$  and *quadratic* when  $s = 2$ .

<sup>5</sup>Here  $\mathbf{C}_j^T \mathbf{C}_j = \mathbf{C}_j \otimes \mathbf{C}_j$  a.k.a. the Kronecker product.

Hence

$$\nabla f(\mathbf{x}) = \sum_{j=1}^m \frac{\mathbf{C}_j^T \mathbf{C}_j \mathbf{x}}{\sqrt{(\mathbf{C}_j \mathbf{x})^2 + \beta}}$$

and the partial derivatives of the Lagrangian  $L(\mathbf{x}, \lambda)$  are

$$\frac{\delta L}{\delta \mathbf{x}} = \sum_{j=1}^m \frac{\mathbf{C}_j^T \mathbf{C}_j \mathbf{x}}{\sqrt{(\mathbf{C}_j \mathbf{x})^2 + \beta}} + \lambda \mathbf{H}^T = 0 \quad (5)$$

$$\frac{\delta L}{\delta \lambda} = \mathbf{H} \mathbf{x} - \mathbf{b} = 0. \quad (6)$$

Thus, the original minimization problem has been transformed into two systems of equations which can be combined to yield the nonlinear system

$$\begin{bmatrix} \mathbf{B}(\mathbf{x}) & \mathbf{H}^T \\ \mathbf{H} & \mathbf{0} \end{bmatrix} \begin{bmatrix} \mathbf{x} \\ \lambda \end{bmatrix} = \begin{bmatrix} \mathbf{0} \\ \mathbf{b} \end{bmatrix} \quad (7)$$

where  $\mathbf{B}(\mathbf{x}) = \sum_{j=1}^m [\mathbf{C}_j^T \mathbf{C}_j / \sqrt{(\mathbf{C}_j \mathbf{x})^2 + \beta}]$ . This system is the generalized Weiszfeld system of Eckhardt [5], [6]. This choice for the matrix  $\mathbf{B}$  enables us to apply this technique to placement with a linear wirelength objective.

To solve this system, we guess an initial approximation  $\mathbf{x}^0$  and solve the system with  $B(\mathbf{x}) = B(\mathbf{x}^0)$ . This solution is called  $\mathbf{x}^1$ , which is the next iterate. In general, we compute the Weiszfeld iterate<sup>6</sup>  $\mathbf{x}^k$  from the previous value  $\mathbf{x}^{k-1}$  by solving the linear system

$$\begin{bmatrix} \mathbf{B}(\mathbf{x}^{k-1}) & \mathbf{H}^T \\ \mathbf{H} & \mathbf{0} \end{bmatrix} \begin{bmatrix} \mathbf{x}^k \\ \lambda \end{bmatrix} = \begin{bmatrix} \mathbf{0} \\ \mathbf{b} \end{bmatrix} \quad (8)$$

which we call the *low-level* system. The iterations continue until a convergence criterion is met. For example, such a criterion may be based on the norm of the *residual vector* [the difference between the left-hand side and the right-hand side of (7)]. This is the main flow of the *generalized Weiszfeld algorithm*.

We now show that this technique is actually the *same* technique used in the GORDIAN-L solver. Recall that GORDIAN-L approximates the linear wirelength objective by a quadratic objective

$$\Phi_L(\mathbf{x}^k) = \sum_{(i,j) \in E} \frac{a_{ij} (x_i^k - x_j^k)^2}{|x_i^{k-1} - x_j^{k-1}|}. \quad (9)$$

Thus, like the generalized Weiszfeld algorithm, GORDIAN-L uses the  $(k-1)$ th iterate to solve for the  $k$ th iterate. Equation (9) can be rewritten as

$$\Phi_L(\mathbf{x}^k) = \sum_{j=1}^m \frac{(\mathbf{C}_j \mathbf{x}^k)^2}{|\mathbf{C}_j \mathbf{x}^{k-1}|}$$

for which the Lagrangian is

$$L(\mathbf{x}^k, \lambda) = \sum_{i=1}^m \frac{(\mathbf{C}_i \mathbf{x}^k)^2}{|\mathbf{C}_i \mathbf{x}^{k-1}|} + \lambda^T (\mathbf{H} \mathbf{x}^k - \mathbf{b})$$

<sup>6</sup>The mathematical idea behind solving (7) is to build an iteration  $\mathbf{x}^k \mapsto \mathbf{x}^{k-1}$  whose fixed point is the unknown solution. Hence, Weiszfeld can be classified as a fixed-point method.

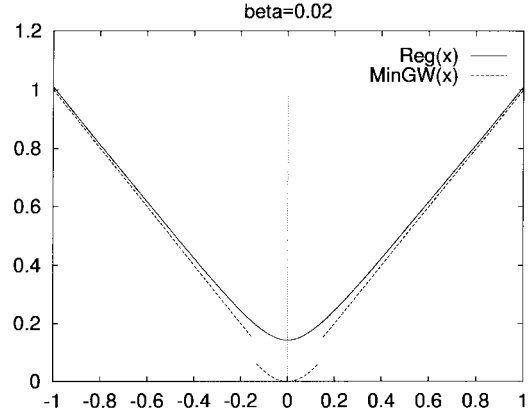


Fig. 3. Comparing the minimal gate width function (MinGW) with the  $\beta$ -regularization (Reg) in one dimension. The original objective is represented by  $|x|$ . Here  $\beta = 0.02$  and the minimal gate width is set to  $\sqrt{\beta} \approx 0.141$ . Note that the discontinuous MinGW has continuous one-sided derivative (optimality conditions), as its branches are given by  $x^2/2\sqrt{\beta}$  and  $|x|$ . By demanding continuity of the objective function and therefore dropping the factor of 1/2, we would make the optimality conditions discontinuous.

and

$$\frac{\delta L}{\delta \mathbf{x}^k} = \sum_{j=1}^m \frac{\mathbf{C}_j^T \mathbf{C}_j \mathbf{x}^k}{|\mathbf{C}_j \mathbf{x}^{k-1}|} + \lambda \mathbf{H}^T = 0. \quad (10)$$

Setting  $\tilde{\mathbf{B}}(\mathbf{x}) = \sum_{j=1}^m (\mathbf{C}_j^T \mathbf{C}_j / |\mathbf{C}_j \mathbf{x}^{k-1}|)$  and using (6), we obtain the same system as in (8) except that the matrix  $\mathbf{B}$  is now replaced with  $\tilde{\mathbf{B}}$ . The only difference between these two matrices is that applying the  $\beta$ -regularization technique approximates  $|\mathbf{C}_j \mathbf{x}|$  with  $\sqrt{(\mathbf{C}_j \mathbf{x})^2 + \beta}$ . This is necessary to avoid numerical problems when  $|x_i^{k-1} - x_j^{k-1}|$  becomes too small (cf., Step 3 of Fig. 2). In GORDIAN-L (see [19]), if this term becomes smaller than the *minimal gate width*, it is replaced with this minimal gate width. In summary, it is simply a matter of using two different schemes ( $\beta$ -regularization versus minimal gate width, cf. Fig. 3) to guarantee reasonable behavior of the solver at the cusps of the objective function. Either scheme can be used with Weiszfeld, and we observe that  $\beta$ -regularization is superior to using minimal gate width: it is closer to the original objective function and its unique minimizer has convenient limit behavior.

*Theorem:* Let  $\Phi_L^\beta$  be the  $\beta$ -regularization of a linear wirelength objective function  $\Phi_L$ , then

- $\lim_{\beta \rightarrow 0} \Phi_L^\beta(\mathbf{x}) = \Phi_L(\mathbf{x})$  uniformly on  $\mathbf{R}^n$ ;
- $\forall \mathbf{x} \in \mathbf{R}^n, \forall \beta_1 > \beta_2 \Phi_L^{\beta_1}(\mathbf{x}) > \Phi_L^{\beta_2}(\mathbf{x}) > \Phi_L^0(\mathbf{x}) = \Phi_L(\mathbf{x})$ ;
- $\lim_{\beta \rightarrow 0} \min_{\mathbf{x} \in \mathbf{R}^n} \Phi_L^\beta(\mathbf{x}) = \min_{\mathbf{x} \in \mathbf{R}^n} \Phi_L(\mathbf{x})$ .

*Proof:* It is enough to prove a) and b) for only one term  $\sqrt{(\mathbf{C}_j \mathbf{x})^2 + \beta}$ . For a) this is done by observing that  $|\Phi_L^\beta - \Phi_L| = \sqrt{\beta}$ , the inequalities b) for one term are true by squaring both sides; c) follows from a) and b).  $\square$

To follow up on the minimal gate width, notice that if one changes the term  $|\mathbf{C}_j \mathbf{x}|$  in the original formulation to  $\max\{|\mathbf{C}_j \mathbf{x}| - t_j, 0\}$ , one gets an equivalent of minimal gate width, as defined in GORDIAN-L, but on a per-edge basis ( $t_j$  can be made quite large if one wishes not to penalize a particular edge once it is shorter than  $t_j$ ). By considering terms of the form  $\max\{0, |x_i - x_j| + |y_i - y_j| - t_{ij}\}$ , one gets a

2-D generalization of the minimal gate width. Both variations of the objection functions need to be  $\beta$ -regularized.

In addition to handling the linear wirelength, the Weiszfeld algorithm can also be applied to the wirelength of an arbitrary real exponent  $p > 1$  by considering terms  $|\mathbf{C}_j \mathbf{x}|^p$  and the like. Indeed, to derive Weiszfeld, we only need to differentiate the objective function (cf., GORDIAN-L whose algorithm relies on a specific form of the obj. function) and  $|x|^p$  is smooth (it is not for  $p = 1$ ), so no  $\beta$ -regularization would be needed.

### B. $\beta$ -Regularization

In our application of the generalized Weiszfeld algorithm to placement with linear wirelength, the objective function was  $\beta$ -regularized to bound the denominator in (5) away from zero. We now highlight properties of the regularized objective function and its relation to the original placement objective function.

By changing all expressions of the form  $|\cdot|$  in the original objective to  $\sqrt{(\cdot)^2 + \beta}$ , the resulting objective becomes strictly convex and therefore has an unique global minimizer. As  $\beta \rightarrow 0$ , this minimizer approaches that of the original linear objective, which in turn can have plenty of minimizers. For example, given a single movable vertex connected to two fixed pads on opposite ends of the layout,  $\Phi_L$  has uncountably many optimal solutions, while the  $\beta$ -regularization will have only one (for  $\beta > 0$ ).

Clearly, as  $\beta$  increases, the disparity between the regularized objective and the original objective increases as well (and the derived solutions will be further from optimal). On the other hand, if  $\beta$  is too small, the derivative of the objective function (which is used in variational methods) will behave badly near points where the original objective is not smooth: matrices in linear systems will become ill-conditioned and solving them will become computationally expensive if not impossible.

The first question is: "How should  $\beta$  be expressed to have comparable effects for various unrelated placement problems?" In the original objective function, all expressions of form  $|\cdot|$  are actually  $|x_i - x_j|$ . These expressions are upper bounded by  $L$ , the length of placement interval which varies across different placement instances. If we set  $\beta = \beta_r L^2$ , where  $\beta_r$  is a small number, then  $\sqrt{(x_i - x_j)^2 + \beta} = L \sqrt{(\tilde{x}_i - \tilde{x}_j)^2 + \beta_r}$  with  $\tilde{x}_i$  and  $\tilde{x}_j$  being on order of  $10^0$  for any placement problem. Our experiments show that in this way we obtain similar behavior for different placement problems if we use the same value of  $\beta_r$ —independent of problem size. We have worked with values ranging from  $10^1$  to  $10^{-7}$ .

The second question, how to choose good values of  $\beta_r$ , is harder; the answer largely depends on how the solutions produced by the Weiszfeld method are used. One can repeatedly solve Weiszfeld for decreasing values of  $\beta$  and stop when the difference between successive placements is small; alternatively, one can stop when the objective function stabilizes. Both strategies can lead to premature stopping, and finding a good heuristic is an open question.

## V. THE PRIMAL-NEWTON METHOD

The Newton approach is often used as a base for developing more sophisticated methods with superlinear convergence

(e.g., in [2], [15]). In this section, we develop what we call the *primal-Newton* method for minimizing the linear wirelength objective. Our main purpose is to introduce the reader to techniques that we will use in developing the *primal-dual Newton* method.<sup>7</sup> Primal-dual will also be a Newton method, but with an additional set of dual variables. Because the primal-dual Newton method converges at least as fast as the primal Newton method and is more stable (i.e., its region of convergence is strictly larger), we do not report experimental data for primal Newton.

Consider minimizing  $\sum_{j=1}^m \sqrt{(\mathbf{C}_j \mathbf{x})^2 + \beta}$  s. t.  $\mathbf{H}\mathbf{x} = \mathbf{b}$ , where the  $k \times n$ -matrix  $\mathbf{H}$  imposes  $k$  constraints on  $n$  cell locations. As before,  $\mathbf{C}_j \in R^n$  contains only two nonzero entries, plus and minus the  $i$ th edge weight, at locations corresponding to the two vertices of the edge.

The Lagrangian for this problem is

$$L(\mathbf{x}, \lambda) = \sum_{j=1}^m \sqrt{(\mathbf{C}_j \mathbf{x})^2 + \beta} + \lambda^T (\mathbf{H}\mathbf{x} - \mathbf{b}). \quad (11)$$

Taking partial derivatives and using (4) gives us

$$\frac{\delta L}{\delta \mathbf{x}} = \sum_{j=1}^m \frac{\mathbf{C}_j^T \mathbf{C}_j \mathbf{x}}{\sqrt{(\mathbf{C}_j \mathbf{x})^2 + \beta}} + \mathbf{H}^T \lambda = 0 \quad (12)$$

$$\frac{\delta L}{\delta \lambda} = \mathbf{H}\mathbf{x} - \mathbf{b} = 0. \quad (13)$$

Applying the Newton method to this nonlinear system, we rewrite the system (invoking the fact that rows of matrix  $\mathbf{C}$  are precisely  $\mathbf{C}_j$  and applying some linear algebra) as follows:

$$\begin{bmatrix} \mathbf{M} & \mathbf{H}^T \\ \mathbf{H} & \mathbf{0} \end{bmatrix} \begin{bmatrix} \delta \mathbf{x} \\ \delta \lambda \end{bmatrix} = - \begin{bmatrix} \mathbf{K}(\mathbf{x}, \lambda) \\ \mathbf{H}\mathbf{x} - \mathbf{b} \end{bmatrix} \quad (14)$$

where

$$\mathbf{M}(\mathbf{x}) = \mathbf{C}^T \mathbf{E}(\mathbf{x})^{-1} \mathbf{F}(\mathbf{x}) \mathbf{C} \quad (15)$$

and the following notation is used.

- $\mathbf{K}(\mathbf{x}, \lambda) = \sum_{j=1}^m [\mathbf{C}_j^T \mathbf{C}_j \mathbf{x} / \sqrt{(\mathbf{C}_j \mathbf{x})^2 + \beta}] + \mathbf{H}^T \lambda$ .
- $\eta_i = \sqrt{(\mathbf{C}_i \mathbf{x})^2 + \beta}$ , with  $\beta$  defined as for the Weiszfeld algorithm.
- $\mathbf{E}(\mathbf{x})$  is an  $m \times m$  diagonal matrix with values in the  $i$ th row equal to  $\eta_i$ .
- $\mathbf{F}(\mathbf{x})$  is an  $m \times m$  diagonal matrix with values in the  $i$ th row equal to  $[1 - (\mathbf{C}_i \mathbf{x})^2 / \eta_i^2]$ .

At the end of each iteration, we update  $\mathbf{x}$  and  $\lambda$  as

$$\begin{aligned} \mathbf{x} &= \mathbf{x} + \delta \mathbf{x} \\ \lambda &= \lambda + \delta \lambda. \end{aligned}$$

Starting with initial values of  $\mathbf{x}$  and  $\lambda$ , we compute corresponding values for  $M(x)$  and  $K(x, \lambda)$ , then update  $\mathbf{x}$  and  $\lambda$  by solving the system in (14). This is repeated until some convergence criterion is met. We call this particular implementation of the Newton method *primal Newton*.

<sup>7</sup>The key issue addressed by primal-dual Newton is global convergence, which primal Newton lacks. No precise mathematical statement about global convergence of primal-dual Newton has been proven, but its reliable convergence properties have been observed in the literature (e.g., [2], [15]) and our experiments.

The primal-Newton method does not possess any kind of global convergence property. Local convergence takes place (a proof can be found in [17]) but we do not know of any estimates of the size of the local convergence region. One can use various globalization techniques (e.g., *line search* and *trust regions*) to guarantee convergence of the primal-Newton method everywhere. However, all of these globalization techniques are known to be inefficient in a number of applications (such as placement and image processing) due to the small size of the region where primal Newton converges quadratically. Modifications to a Newton method which allow it to achieve global convergence can be found in [15] where a corresponding theorem is proven and numerical results demonstrating advantages over the Weiszfeld method are shown. Reference [15] also contains a discussion of *degeneracy*, a feature of some placement problems for which Newton-like methods are only linearly convergent.

The various considerations related to top-level stopping criteria for Weiszfeld in the previous section do not carry over to the Newton method since we are searching for  $\mathbf{x}$  which cannot be characterized as satisfying a particular linear system. In other words, we do not have an analogue for the residual norm. However, convergence criteria in terms of successive iterates are easily defined since  $\delta\mathbf{x}$  is the difference between successive iterates. Alternatively, various convergence criteria can be deduced from the observation that the *nonlinear residual*, the right-hand side of (14), goes to zero as the Newton method progresses.

## VI. THE PRIMAL-DUAL NEWTON METHOD

The idea of the primal-dual Newton approach was developed by Conn and Overton in [4] and has been recently used for a denoising application in image processing (see [2]). Numerical results suggest that the approach has fast convergence, stability, and significant practical value.

Recall that the optimization problem we will solve is: find  $\mathbf{x}$  which minimizes

$$f(\mathbf{x}) = \sum_{j=1}^m \sqrt{(\mathbf{C}_j\mathbf{x})^2 + \beta} \quad \text{s.t. } \mathbf{H}\mathbf{x} = \mathbf{b} \quad (16)$$

where  $\mathbf{C}_j \in R^n$  again contains only two nonzero entries, plus and minus the  $i$ th edge weight, at locations corresponding to the two vertices of the edge.  $\mathbf{H}$  is a  $k \times n$ -matrix imposing  $k$  constraints on  $n$  cell locations.

Let  $s_j = \mathbf{C}_j\mathbf{x}$ . Then we can rewrite (16) as: find  $\mathbf{x}$  which minimizes

$$\sum_{j=1}^m \sqrt{s_j^2 + \beta} \quad \text{s.t. } \mathbf{C}_j\mathbf{x} - s_j = 0 \text{ and } \mathbf{H}\mathbf{x} = \mathbf{b}. \quad (17)$$

The Lagrangian for this problem is

$$L(\mathbf{x}, \mathbf{s}, \mathbf{z}, \lambda) = \sum_{j=1}^m \sqrt{s_j^2 + \beta} + \sum_{j=1}^m z_j(\mathbf{C}_j\mathbf{x} - s_j) + \lambda(\mathbf{H}\mathbf{x} - \mathbf{b})$$

where  $\lambda$  and  $\mathbf{z}$  are the Lagrange multipliers for  $\mathbf{x}$  and  $\mathbf{s}$ . The Karush–Kuhn–Tucker first order necessary conditions are

$$\frac{\partial L}{\partial \mathbf{x}} = \sum_{j=1}^m \mathbf{C}_j^T z_j + \mathbf{H}^T \lambda = 0 \quad (18)$$

$$\frac{\partial L}{\partial s_j} = \frac{s_j}{\sqrt{s_j^2 + \beta}} - z_j = 0, \quad j = 1, \dots, m \quad (19)$$

$$\frac{\partial L}{\partial z_j} = \mathbf{C}_j\mathbf{x} - s_j = 0, \quad j = 1, \dots, m \quad (20)$$

$$\frac{\partial L}{\partial \lambda} = \mathbf{H}\mathbf{x} - \mathbf{b} = 0. \quad (21)$$

Using (20) to eliminate  $s_j$  from (19) and rearranging slightly

$$\sum_{j=1}^m \mathbf{C}_j^T z_j + \mathbf{H}^T \lambda = 0 \quad (22)$$

$$\mathbf{C}_j\mathbf{x} - \left[ \sqrt{(\mathbf{C}_j\mathbf{x})^2 + \beta} \right] z_j = 0, \quad j = 1, \dots, m \quad (23)$$

$$\mathbf{H}\mathbf{x} - \mathbf{b} = 0. \quad (24)$$

We can now apply Newton's method to this nonlinear system. Differentiating the left-hand side of (22) with respect to  $\mathbf{z}$  and writing the result as a matrix, we get  $\mathbf{C}^T$  (because  $\mathbf{C}^T$  is composed of  $\mathbf{C}_j^T$ ). Differentiating the left-hand side of (23) with respect to  $\mathbf{x}$ , we get [refer to (4)]

$$\mathbf{C}_j - \frac{z_j(\mathbf{x}^T \mathbf{C}_j^T) \mathbf{C}_j}{\sqrt{(\mathbf{C}_j\mathbf{x})^2 + \beta}}, \quad j = 1, \dots, m \quad (25)$$

which can be rewritten in matrix form as

$$\mathbf{I}(\mathbf{z}, \mathbf{x})\mathbf{C} \quad (26)$$

with

$$\mathbf{I}(\mathbf{z}, \mathbf{x}) = \text{diag} \left[ 1 - \frac{z_i(\mathbf{x}^T \mathbf{C}_i^T)}{\eta_i} \right]$$

$$\eta_j = \sqrt{(\mathbf{C}_j\mathbf{x})^2 + \beta}.$$

We set  $\mathbf{E} = \text{diag}(\eta_i)$ .

Finally, the Newton method gives the following linear system<sup>8</sup> which we need to solve repeatedly

$$\begin{bmatrix} \mathbf{C}^T & 0 & \mathbf{H}^T \\ -\mathbf{E} & \mathbf{I}(\mathbf{z}, \mathbf{x})\mathbf{C} & 0 \\ 0 & \mathbf{H} & 0 \end{bmatrix} \begin{bmatrix} \delta\mathbf{z} \\ \delta\mathbf{x} \\ \delta\lambda \end{bmatrix} = - \begin{bmatrix} \mathbf{C}^T\mathbf{z} + \mathbf{H}^T\lambda \\ \mathbf{C}\mathbf{x} - \mathbf{E}\mathbf{z} \\ \mathbf{H}\mathbf{x} - \mathbf{b} \end{bmatrix}. \quad (27)$$

To reduce the dimension of this system, we eliminate  $\delta\mathbf{z}$  by substituting its second equation

$$\delta\mathbf{z} = -\mathbf{z} + \mathbf{E}(\mathbf{x})^{-1}\mathbf{C}\mathbf{x} + \mathbf{E}(\mathbf{x})^{-1}\mathbf{I}(\mathbf{z}, \mathbf{x})\mathbf{C}\delta\mathbf{x} \quad (28)$$

into the first equation. After cancellation, we get

$$\mathbf{C}^T\mathbf{E}^{-1}\mathbf{I}(\mathbf{z}, \mathbf{x})\mathbf{C}\delta\mathbf{x} + \mathbf{H}^T\delta\lambda = -(\mathbf{C}^T\mathbf{E}^{-1}\mathbf{C}\mathbf{x} + \mathbf{H}^T\lambda)$$

<sup>8</sup>Here dual variable  $\mathbf{z}$  and matrices  $\mathbf{E}$ ,  $\mathbf{I}$  are  $m$ -dimensional,  $\mathbf{x}$  and  $\mathbf{b}$  are  $n$ -dimensional, while  $\lambda$  is  $k$ -dimensional.  $\mathbf{H}$  and  $\mathbf{C}$  have sizes  $k \times n$  and  $m \times n$ , respectively.

and together with the third equation of (27) this makes

$$\begin{bmatrix} \mathbf{C}^T \mathbf{E}(\mathbf{x})^{-1} \mathbf{I}(\mathbf{z}, \mathbf{x}) \mathbf{C} & \mathbf{H}^T \\ \mathbf{H} & 0 \end{bmatrix} \begin{pmatrix} \delta \mathbf{x} \\ \delta \lambda \end{pmatrix} = - \begin{bmatrix} \mathbf{K}(\mathbf{x}, \lambda) \\ \mathbf{H} \mathbf{x} - \mathbf{b} \end{bmatrix} \quad (29)$$

where<sup>9</sup>

$$\begin{aligned} \mathbf{K}(\mathbf{x}, \lambda) &= \mathbf{C}^T \mathbf{E}^{-1} \mathbf{C} \mathbf{x} + \mathbf{H}^T \lambda \\ &= \sum_{j=1}^m \frac{\mathbf{C}_j^T \mathbf{C}_j \mathbf{x}}{\eta_j} + \mathbf{H}^T \lambda. \end{aligned} \quad (30)$$

In the overall algorithm,  $\delta \mathbf{z}$  gives an *update direction* for  $\mathbf{z}$ , and we are free to use  $\delta \mathbf{z}$  with any factor we want. However, as noted in [2], for the matrix in (29) to be nonsingular one requires  $\|\mathbf{z}^k\|_\infty \leq 1$ . To ensure this, iterates  $\mathbf{z}^k$  of the *dual* variable are defined recursively with  $\mathbf{z}^0 = \mathbf{0}$ , and updates computed at each iteration by (28) and the *line search* formula  $\mathbf{z}^{k+1} = \mathbf{z}^k + S \delta \mathbf{z}$  where

$$S = \min\{0.9 \sup\{S \mid \|\mathbf{z}^k + S \delta \mathbf{z}\|_\infty < 1\}, 1\}. \quad (31)$$

One computes the supremum by looping over coordinates and solving  $-1 \leq \mathbf{z}^k + S \delta \mathbf{z} \leq 1$  for  $S$ . (In practice,  $S \rightarrow 1$  as iterates converge, and we find that  $S = 1$  for most iterates.) The variables  $\mathbf{x}$  and  $\lambda$  are updated at each iteration using

$$\begin{aligned} \mathbf{x} &= \mathbf{x} + \delta \mathbf{x} \\ \lambda &= \lambda + \delta \lambda. \end{aligned}$$

Computationally, we deal with the system (29) just as with the primal-Newton method for the linear objective in Section V. To find an initial approximation close to the quadratic convergence region, one can solve a few linear systems as if using the Weiszfeld algorithm, then switch to primal-dual iterations. This may be applied as a possible speedup since (as the experimental results below show) the Weiszfeld algorithm can find a rough approximation faster than primal dual.

The right-hand side of (29) goes to zero as top-level iterates converge. This means that all convergence tests involving residual vectors should be formulated in terms of *relative tolerance* or should otherwise depend on the right-hand side of the system. We have observed in our experiments that if for some reason (29) is not solved precisely enough, Newton top-level iterates can start to diverge.

The remarks given for the primal-Newton method above also apply to primal-dual Newton (see [2]); in particular, primal-dual Newton possesses quadratic convergence (see [12, 5.4.1]) and is preferable to the linearly convergent Weiszfeld algorithm. Primal-dual Newton converges quadratically in strictly larger regions than the Newton method and is only 30–50% more expensive in computation and memory per iteration than the Weiszfeld method.

<sup>9</sup>The second equality in (30) relies on  $\mathbf{Q} = -\mathbf{C}_0^T \mathbf{W} \mathbf{C}_0$ , which expresses the *Laplacian*  $\mathbf{Q}$  in terms of the *pure* (i.e., having only 0, 1, and  $-1$  entries) *incidence matrix*  $\mathbf{C}$  and the *weight matrix*  $\mathbf{W}$ . In the simple case where the edge weights of the original graph are all 1,  $\sum_{j=1}^m (\mathbf{C}_j^T \mathbf{C}_j / \eta_j)$  can be interpreted as the negative Laplacian of the graph with connectivity matrix  $\mathbf{C}$  and edge weights given by  $\eta_j^{-1}$ . (Here,  $\mathbf{E} = \mathbf{W}$ .) The general case can be reduced to the simple case by writing  $\mathbf{C} = \mathbf{W} \mathbf{C}_0$ .

## VII. EXPERIMENTAL VALIDATION

We now describe our experimental methodology and present experimental results which confirm the efficiency of primal-dual Newton in comparison to the generalized Weiszfeld with  $\beta$ -regularization. Since the generalized Weiszfeld method is equivalent to the GORDIAN-L numerical engine for very small values of  $\beta$ , our experiments show that primal-dual Newton is superior to the GORDIAN-L solver for placement with a linear objective.

### A. Implementing the Low-Level Solver

We implemented the Weiszfeld and primal-dual Newton iterations within our own sparse-matrix testbed; this testbed is coupled to a design database and partitioning and layout tools, with interfaces via standard design interchange formats. Thus, we were able to verify our methods using standard benchmarks from the literature (ftp to cbl.ncsu.edu).<sup>10</sup>

When implementing the primal-dual method, it is crucial to solve the linear system (29) precisely enough that the top-level iterates will converge. One finds that matrices arising in (29) are usually much denser and more ill-conditioned than in analogous systems arising from denoising problems in image processing or from the numerical solution of partial differential equations. This makes it harder for any low-level solver to find sufficiently precise approximate solutions. To avoid undue loss of sparsity when  $\mathcal{O}(p^2)$  edges are introduced for some very large  $p$ -pin net, we represent any large net with  $>100$  pins by a random cycle through its cells.<sup>11</sup>

Since our implementation is designed to accommodate examples of any size, we use iterative solvers, specifically, GMRES or BICGSTAB with ILU preconditioner.<sup>12</sup> Here, we must refer the reader to [12, Ch. 6], where usage of iterative (inexact) solvers is considered with special regard to Newton methods. Our solver changes the values of relative tolerance according to the rule in (6.18) of [12], using parameters  $\gamma = 0.5$  and  $\eta_{\text{Max}} = 10^{-4}$  in that rule.

<sup>10</sup>Our implementations are in part (e.g., for sparse-matrix BLAS) based on the Portable, Extensible Toolkit for Scientific computation (PETSc) library; this is free software developed and maintained at Argonne National Laboratory [1]. Salient features of PETSc include the following: 1) PETSc is an object-oriented library which can be linked to Fortran, C, and C++ programs. It supports several sparse matrix formats, basic linear algebra for them, matrix factorization, matrix reordering, and various linear system solvers; 2) PETSc is designed for multiprocessors and uses the message passing interface (MPI), however, we mostly used it on uniprocessor workstations; 3) PETSc has error reporting and profiling capabilities. It can also report performance and diagnostic information such as memory usage and number of floating point operations executed. It supports graphics, has several GUI tools for the X-window environment, and is ported to a variety of UNIX-like operating systems (we used it on SunOS, Solaris and Linux); 4) thorough documentation is available for PETSc, and its solvers were the fastest of what we have tested.

<sup>11</sup>Note that the graph representation of the netlist must be connected, e.g., when using an ILU preconditioner.

<sup>12</sup>For better results with examples of small size (say, under 1000 cells), one can solve the linear systems (7) and (29) directly; this limit can be increased if matrices are sparser. Also note that matrices arising from (7) and (29) are always symmetric and semidefinite. Thus, other Krylov Subspace methods which can be used here are BICGSTAB, QMR, SYMMLQ, etc.

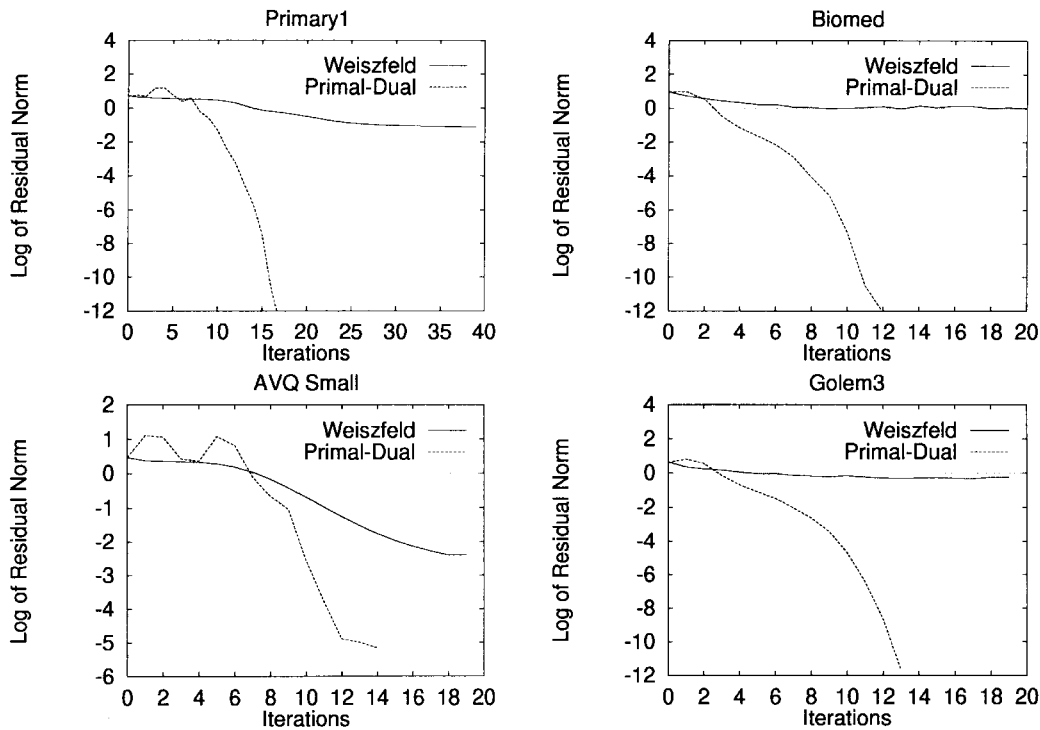


Fig. 4. Comparison between convergence of primal-dual and Weiszfeld.

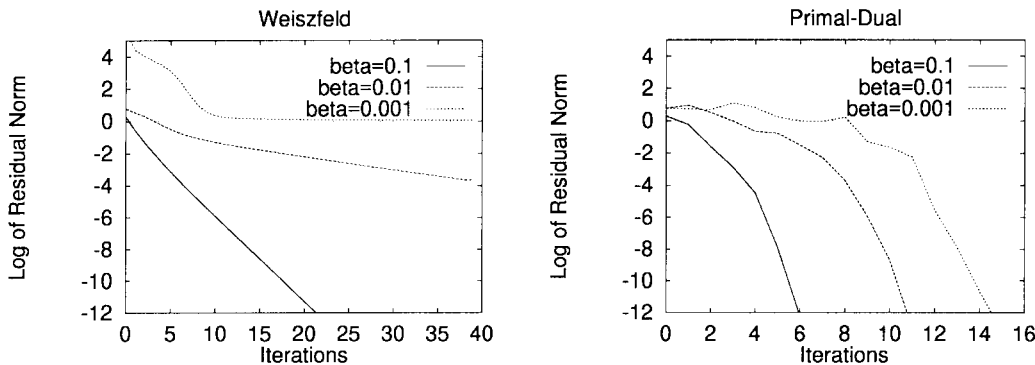
Fig. 5. Dependence of convergence (Primary1 benchmark) on the value of  $\beta_r$  used ( $10^{-1}$ ,  $10^{-2}$ , and  $10^{-3}$ ). We plot  $\log_{10}$  of  $L_2$  norm of the nonlinear residual versus the number of top-level iterations.

TABLE I  
TEST EXAMPLES FOR PD VERSUS WEISZFELD COMPARISON.  
VLSI BENCHMARK CIRCUITS USED IN COMPARING THE  
WEISZFELD AND PRIMAL-DUAL NEWTON METHODS

Test Case	Pads	Cells	Nets
primary1	107	752	704
biomed	97	6417	6442
avq_small	64	21854	21884
golem3	2767	100281	144949

### B. Convergence of Primal-Dual Newton and Weiszfeld Methods

We now give experimental evidence showing that the primal-dual Newton iteration achieves quadratic convergence. Fig. 4 compares its convergence behavior with that of Weiszfeld algorithm on standard benchmarks (see Table I) maintained by the CAD Benchmarking Laboratory. While our

implementation is not yet optimized for speed, runtimes for the avq\_small test case are still only on the order of 7 CPU seconds per Weiszfeld iteration on a 140 MHz Sun Ultra-1. Note that iterations can be sped up considerably if we relax accuracy requirements in the solver and preconditioner. In general, many control parameters allow tradeoffs between solution quality and runtime.

In all of our tests, the residual norm tends to converge linearly in the beginning, although not always monotonically. However, when primal-dual iterates near the optimal solution, their residual norm converges *quadratically*. At the same time, the Weiszfeld method shows *linear* convergence everywhere. We stop the top-level iterations when the nonlinear residual has decreased by a prescribed factor ( $10^{-13}$  in this experiment), or when the iteration count reaches 40. The  $\beta_r$  value we used was  $10^{-4}$ .

We discovered (Fig. 5) that more iterations are needed to reach the quadratic convergence region for smaller  $\beta_r$  values.

However, the difference in convergence behavior between the two algorithms is more apparent for smaller  $\beta_r$  values.

### VIII. CONCLUSIONS

As shown in the previous section, the Weiszfeld algorithm corresponding to GORDIAN-L is at best linearly convergent, while primal-dual Newton provides robust quadratic convergence.

We note that the original Weiszfeld formulation is in fact much weaker than what we have developed (in the original work, only one point is placed and there is no concept of  $\beta$ -regularization). Our generalization and underlying formulation have significant theoretical value in that they allow derivation of a large family of effective global optimization methods in an uniform mathematical setting. We have recently begun integration of the primal-dual Newton algorithm to address linear wirelength minimization and a variety of alternate objectives within a standard-cell placement engine.

### REFERENCES

- [1] *PETSc 2.0 User's Manual*, Argonne National Laboratory, S. Balay, W. Gropp, L. C. McInnes, and B. Smith, 1995 [Online]. Available WWW: <http://www.mcs.anl.gov/petsc/petsc.html>.
- [2] T. F. Chan, G. H. Golub, and P. Mulet, "A nonlinear primal-dual method for TV-based image restoration," in *Proc. ICAOS'96, 12th Int. Conf. Analysis Optimization Syst.: Images, Wavelets, PDE's*, (Lecture Notes in Control and Information Sciences), M. Berger *et al.* Eds., Paris, France, June 26–28, 1996, no. 219, pp. 241–252.
- [3] C. K. Cheng and E. S. Kuh, "Module placement based on resistive network optimization," *IEEE Trans. Computer-Aided Design*, vol. CAD-3, pp. 218–225, 1984.
- [4] A. Conn and M. Overton, "A primal-dual interior point method for minimizing a sum of euclidean distances," Computer Science Department, New York University, Tech. Rep., 1995.
- [5] U. Eckhardt, "On an optimization problem related to minimal surfaces with obstacles," in *Optimization and Optimal Control*, (Lecture Notes in Mathematics), R. Bulirsch, W. Oetti, and J. Stoer, Eds. New York: Springer-Verlag, 1975, pp. 95–101.
- [6] ———, "Weber's problem and Weiszfeld's algorithm in general spaces," *Math. Programming*, vol. 18, pp. 186–196, 1980.
- [7] W. C. Elmore, "The transient response of damped linear network with particular regard to wideband amplifiers," *J. Appl. Physics*, vol. 19, pp. 55–63, 1948.
- [8] K. Fukunaga, S. Yamada, H. S. Stone, and T. Kasai, "Placement of circuit modules using a graph space approach," in *Proc. 20th ACM/IEEE Design Autom. Conf.*, 1983, pp. 465–471.
- [9] W. Hackbush, *Iterative Solution of Large Sparse Systems*. New York: Springer-Verlag, 1994.
- [10] L. Hagen and A. B. Kahng, "Improving the quadratic objective function in module placement," in *Proc. IEEE Int. ASIC Conf. Exhibit*, Rochester, NY, Sept. 1992, pp. 21–25.
- [11] T. Hamada, C.-K. Cheng, and P. M. Chau, "Prime: A timing-driven placement tool using a piecewise linear resistive network approach," in *Proc. 30th ACM/IEEE Design Autom. Conf.*, 1993, pp. 531–536.
- [12] C. Kelley, "Iterative methods for linear and nonlinear equations," in *Frontiers in Applied Mathematics*, vol. 16. Philadelphia, PA: SIAM Press, 1995.
- [13] J. Kleinhans, G. Sigl, F. Johannes, and K. Antreich, "GORDIAN: VLSI placement by quadratic programming and slicing optimization," *IEEE Trans. Computer-Aided Design*, vol. 10, pp. 356–365, Mar. 1991.
- [14] J. Li, J. Lillis, L.-T. Liu, and C.-K. Cheng, "New spectral linear placement and clustering approach," in *Proc. 33rd ACM/IEEE Design Autom. Conf.*, 1996, pp. 88–93.
- [15] Y. Li, A Newton acceleration of the Weiszfeld algorithm for minimizing the sum of Euclidean distances," Cornell University, Tech. Rep., 1996.
- [16] I. I. Mahmoud, K. Asakura, T. Nishibu, and T. Ohtsuki, "Experimental appraisal of linear and quadratic objective functions effect on force directed method for analog placement," *IEICE Trans. Fundamentals of Electron., Commun. Comput. Sci.*, vol. E77-A, no. 4, pp. 719–725, Apr. 1994.
- [17] J. M. Ortega and W. C. Rheinboldt, *Iterative Solution of Nonlinear Equations in Several Variables*. New York: Academic, 1970.
- [18] B. M. Riess, K. Doll, and F. M. Johannes, "Partitioning very large circuits using analytical placement techniques," in *Proc. 31st ACM/IEEE Design Autom. Conf.*, 1994, pp. 646–651.
- [19] G. Sigl, K. Doll, and F. Johannes, "Analytical placement: A linear or a quadratic objective function?," in *Proc. 28th ACM/IEEE Design Autom. Conf.*, 1991, pp. 427–432.
- [20] W. Swartz and C. Sechen, "Timing driven placement for large standard cell circuits," in *Proc. 32nd ACM/IEEE Design Autom. Conf.*, 1995, pp. 211–215.
- [21] R. S. Tsay and E. Kuh, "A unified approach to partitioning and placement," *IEEE Trans. Circuits Syst.*, vol. 38, pp. 521–633, May 1991.
- [22] E. Weiszfeld, "Sur le Point pour Lequel la Somme des Distances de  $n$  Points Donnés est Minimum," *J. Tôhoku Math.* vol. 43, pp. 355–386, 1937.
- [23] G. J. Wipfler, M. Wiesel, and D. A. Mlynski, "A combined force and cut algorithm for hierarchical VLSI layout," in *Proc. 20th ACM/IEEE Design Autom. Conf.*, 1983, pp. 124–125.



**Charles J. Alpert** (M'93) received the B.S. degree in math and computational sciences and the B.A. degree in history from Stanford University in 1991. He received the Ph.D. degree in computer science at the University of California at Los Angeles in 1996.

In 1996, he became a Research Staff Member for the Computer Aided Design Group at the IBM Austin Research Laboratory in Austin, TX. His research interests include partitioning, placement, routing, interconnect optimization, and clocking.

Dr. Alpert received two Best Paper Awards at the 1994 and 1995 ACM/IEEE Design Automation Conferences.



**Tony F. Chan** received the B.S. degree in engineering in 1973 and the M.S. degree in aerospace engineering in 1975 from the California Institute of Technology, Pasadena. He received the Ph.D. degree in computer science from Stanford University, California, in 1978.

He is currently the Chair of the Mathematics Department at the University of California, Los Angeles, where he has been a Professor since 1986. His research interests include the design of efficient computational algorithms for large scale scientific computing (e.g., multigrid and domain decomposition algorithms, iterative methods, Krylov subspace methods, and parallel algorithms), VLSI circuit placement, and PDE methods for image processing.

**Andrew B. Kahng** (A'89), for a photograph and biography, see this issue, p. 1.



**Igor L. Markov** (S'96) was born in March 1973 in Kiev, Ukraine. He received the B.A. degree in mathematics from Kiev University, Ukraine, and the M.A. degree in mathematics from the University of California, Los Angeles. He is currently in the Ph.D. program in pure mathematics at the University of California, Los Angeles.

Presently he is a member of the VLSI CAD laboratory in the Computer Science Department at the University of California, Los Angeles. His research interests in pure mathematics include operator algebra and its applications to noncommutative geometry and topology as well as computational sciences. Applied research interests include computer-aided design of VLSI circuits, the theory of global optimization, the interplay between discrete and continuous algorithms, as well as software design management.

Mr. Markov is a member of AMS.



**Pep Mulet** (M<sup>92</sup>) was born in Gata, Spain, in 1966. He received the M.S. and the Ph.D. degrees in mathematics from the University of Valencia, Spain, in 1989 and 1992, respectively.

He benefited from a fellowship in the Department of Algebra of the University of Valencia from 1990 to 1993 and a post-doctoral position at the Department of Mathematics of the University of California, Los Angeles, from 1995 to 1996. Since 1995, he has been an Assistant Professor at the Department of Applied Mathematics of the University of Valencia. His current research interests include image processing, especially image restoration, computational linear algebra, optimization, and parallel algorithms.